Available online at www.sciencedirect.com
SCIENCE DIRECT
Carbon 44 (2006) 1790–1800
CARBON
www.elsevier.com/locate/carbon

Analysis of gas phase compounds in chemical vapor deposition of carbon from light hydrocarbons

Koyo Norinaga, Olaf Deutschmann *, Klaus J. Hüttinger

Institut für Technische Chemie und Polymerchemie, Universität Karlsruhe, Engesserstr. 20, 76131 Karlsruhe, Germany

Received 22 July 2005; accepted 23 December 2005
Available online 7 March 2006

Abstract

Product distributions in the pyrolysis of ethylene, acetylene, and propylene are studied to obtain an experimental database for a detailed kinetic modeling of gas phase reactions in chemical vapor deposition of carbon from these light hydrocarbons. Experiments were performed with a vertical flow reactor at 900 °C and pressures from 2 to 15 kPa. Gas phase components were analyzed by both on-line and off-line gas chromatography. More than 40 compounds from hydrogen to coronene were identified and quantitatively determined as a function of the residence time varied up to 1.6 s. Product recoveries were generally more than 90%. Analysis of the kinetics of the conversion of the hydrocarbons resulted in global reaction orders of 1.2 (ethylene), 2.7 (acetylene), and 1.5 (propylene). First order dehydrogenation reactions and third order trimerization reactions leading to benzene are decisive reactions for ethylene and acetylene, respectively. Conversion of propylene should also be based on two simultaneous reactions, a first order dissociation reaction, and second order reactions such as bimolecular reaction of propylene resulting an allyl and a propyl radical. These insights should be useful to develop a reaction mechanism based on elementary reactions in forthcoming studies.

Keywords: Pyrolytic carbon; Chemical vapor deposition; Pyrolysis; Chromatography; Reaction kinetics

1. Introduction

Chemical vapor deposition (CVD) of carbon from light hydrocarbons is mainly used in the production of carbon fiber reinforced carbon (CFC) by infiltrating pyrolytic carbon into carbon fiber performs [1]. The CVD of carbon involves simultaneous processes of complex gas-phase reactions leading to various products including polycyclic aromatic hydrocarbons (PAHs) and soot, and heterogeneous reactions leading to the deposition of pyrolytic carbon on the substrate surface [2,3]. Therefore, the overall kinetics of the deposition process is determined by the kinetics of gas-phase and surface reactions and in particular the interaction or competition of gas-phase and surface reactions. A great variety of hydrocarbons and hydrocarbon radicals are formed by gas phase reactions, and any of these species has a potential for chemisorption or physisorption on the growing carbon surface and thus to form pyrolytic carbon. These complications make it difficult to understand the CVD of carbon quantitatively and to develop a precise model.

Becker and Hüttinger proposed a simplified model which can describe the kinetics of carbon deposition from C_2 hydrocarbons [4]. A lumping approach was used in which a large number of gas phase species are lumped into three groups, i.e. C_2, C_4, and C_6 hydrocarbons, and the rate constants of the chemical reactions involved are estimated by a numerical fitting. This model was successfully used for simulation of the chemical vapor infiltration (CVI) process [5,6]; it can also serve as useful benchmark for detailed kinetic schemes.

It is a challenge for future research to advance from the traditional lumping method and to develop a model based on elementary reactions which describes the complex gas

* Corresponding author. Tel.: +49 721 608 3138; fax: +49 721 608 4805.
E-mail address: deutschmann@ict.uni-karlsruhe.de (O. Deutschmann).

0008-6223/$ - see front matter © 2006 Elsevier Ltd. All rights reserved.
doi:10.1016/j.carbon.2005.12.050

phase chemistry of CVD of carbon at a molecular level. A numerical simulation of CVI based on the detailed chemical kinetics and correlation between kinetics and structures of pyrolytic carbon is necessary to develop and optimize the CFC production process. A great number of studies can be found in literatures for the pyrolysis of hydrocarbons such as ethylene [7–27], acetylene [28–56], and propylene [57–76]. Most of the studies are focused on pyrolysis mechanism at initial stages with shock tube at very short residence times or volume reactor at low temperatures. Although a variety of gas phase products were found in CVD of pyrolytic carbon [77,78], experimental results on the hydrocarbon pyrolysis with a wide range of products analysis including large polycyclic aromatic hydrocarbons and pyrolytic carbon are very few. Results obtained at reduced pressures without diluent inert gas, which are employed in CFC production process to gain favorable free gas diffusion, are also insufficient.

Descamps et al. [79] developed a gas phase reaction mechanism (53 species and 205 reactions) in CVD of carbon from propane using elementary reactions reported in the literature. The mechanism was validated by comparing the computations with the experimental data on the gas phase compositions obtained at 2 kPa and two temperatures of 800 and 1000 °C. In situ Fourier transform infrared spectroscopy was employed to determine the concentrations of gas phase components [80,81]. Since their analysis was semi-quantitative, their mechanism validation is likely to be insufficient. Detailed and quantitative information on the gas phase components in hydrocarbon pyrolysis at conditions relevant to CVD of carbon is still limited.

Experimental data on the gas phase compositions which are evaluated quantitatively are needed for the development of a more accurate elementary-step like gas phase reaction mechanism. Experiments at well-defined conditions with satisfying material balances are the fundamental requirements. Furthermore, experimental results obtained from various source hydrocarbons are useful to develop a comprehensive mechanism. In this study, the species composition in the gas phase in CVD of carbon from the unsaturated light hydrocarbons ethylene, acetylene, and propylene is analyzed quantitatively. The CVD experiments were performed in a vertical flow reactor. The temperature was 900 °C, pressure was varied from 2 to 15 kPa, and the effective residence time from 0.1 to 1.6 s. Gaseous and condensing products were analyzed using on-line and off-line gas chromatography, respectively.

2. Experimental

The experimental set-up is given in the Supplementary data. The reactor is identical to that used in a previous study [82]. Total length of the reactor is 440 mm. The deposition space is located at the center of the reactor and formed by a cylindrically shaped alumina ceramic tube, 22 mm i.d. and 40 mm long. A channel structure, made out of cordierite, with 400 channels per square inch is fitted in the alumina ceramic tube, resulting in a relatively high surface area/volume ratio of the deposition space $[A/V]$ of 3.2 mm^{-1}. The inlet and outlet tubes (8 mm i.d.) are connected to the deposition space through conical inlet and outlet nozzles. These narrow tubes increase linear velocity of flowing gas, reducing the predecomposition of the hydrocarbon gas and post reactions beyond the reaction zone. The nozzles are employed to generate a plug-flow [4] which is necessary to obtain reliable kinetic data. Temperature profile for the reactor was measured under an argon flow with a type K thermocouple (Rössel Messtechnik GmbH & Co.) that was moved axially along the reactor length. The measured temperature profile for a set point temperature of 900 °C can be found in the Supplementary data. The axial temperature variation of the deposition space is within ±2 K of the target temperature.

Previous simulation for gas temperature in the reactor applied [83] suggests that the channel structures can effectively homogenize the temperature in the radial direction. Influences of reaction enthalpies on the temperature profiles in axial direction lead to some uncertainties. In ongoing research their effects are studied more accurately by CFD simulations coupled with detailed chemical reaction schemes [84].

The deposition experiments were performed at a temperature of 900 °C, pressures ranging from 2 to 15 kPa and effective residence times of up to 1.6 s. Ethylene, acetylene, and propylene with respective purities higher than 99.4%, 99.6%, and 99.5% were all purchased from Air Liquid Co. Ltd. and used as carbon sources.

The chemically reacting flow leads to density variations along the axial coordinate, which introduces some uncertainties in the estimation of the residence time. The residence time, τ, without taking into account these density changes, here simply derived from

$$\tau = V_R / v_u \tag{1}$$

with V_R = free volume of the deposition space in m^3; v_u = the upstream volumetric flow rate of the hydrocarbon gases in m^3/s at the deposition temperature, and pressure. Pyrolysis of the hydrocarbons changes the gas density and hence the volumetric flow rate downstream. A corrected flow rate, v_d is therefore used:

$$v_d = v_u * \varepsilon \tag{2}$$

where ε is the volume expansion factor, ε, which is calculated by

$$\varepsilon = v_{out} / v_{in} \tag{3}$$

where v_{out} and v_{in} are the volumetric flow rate at reactor outlet and inlet, respectively, at ambient conditions. The measurement of ε is based on the displacement of a given volume of water per unit of time. Liquid products which would condense at water temperature will cause under-estimations of the exit flow rates. Nevertheless the v_{out} measurement is necessary to calculate the gaseous product yields as well as to establish a perfect material balance. The effective residence time, τ_{eff}, was thus defined by

$$\tau_{\text{eff}} = V_{\text{R}}/v_{\text{d}} = \tau/\varepsilon \quad (4)$$

It is impossible to estimate a real or a mean residence time since the residence time distributions are currently not clear. However, it is noted that τ and τ_{eff} represent two extremes of the residence time and the real residence time should lie in between. The CFD simulations coupled with detailed chemical reaction schemes are currently in progress and will help to evaluate the flow rate profile in the reactor accurately.

Gaseous products up to C_4 compounds were analyzed on-line with a Sichromat 3 gas chromatograph (Siemens) equipped with a vacuum dosing system. A Porapak N column (Chrompak) and a thermal conductivity detector were used for separation and peak detection, respectively.

Liquid products larger than benzene were collected in two cold traps set at 195 K, dissolved in a measured amount of acetone and analyzed by a Sichromat 1–4 gas chromatograph (Siemens) equipped with a capillary column (CP-Sil 8 CB LB/MS, Chrompak) and a flame ionization detector. Species were identified by the retention time matching. Details of the analysis of liquid products and a typical chromatogram are given elsewhere [78]. Our previous work of gas phase analysis using methane as a precursor gas [85] indicates that the perfect collection of the products was very difficult with a cold trap after the reactor outlet in CVD experiments at low pressures. The cold trap after the membrane vacuum pump was found to be useful to collect light aromatic hydrocarbons such as benzene and naphthalene and thus enabled to improve the material balances of the analysis. Flexible heaters were maintained at 443 K to avoid condensation and adsorption of products on inner walls. On-line gas phase analysis and off-line analysis of liquid products were performed in separate runs. The relative errors of the product yield generally within ±5% and ±20% for the yields of gaseous and condensing products, respectively.

3. Results and discussion

3.1. Compounds found in gas phase

Fig. 1 shows the chemical structures of the compounds found in the gas phase. More than 40 species ranging from hydrogen to coronene could be identified and quantitatively determined as a function of both pressure and residence time. 1-Butene is observed only in the CVD from propylene. Propylene and 1,3-butadiene are not found in the CVD from acetylene. Xylenes and ethylbenzene peaks could not be distinguished. Besides these compounds diacetylene (C_4H_2) and propynylbenzene are observed in the CVD from propane [81]. The aromatic compounds found in the present experiments are identical with those found in our previous CVD experiments at 1100 °C and 5–60 kPa using methane as precursor gas [78]. Propane pyrolysis at 950 °C and 2 kPa [81] as well as ethane pyrolysis at 912 °C and 40 kPa also produce identical aromatic compounds [77]. Polycyclic aromatic hydrocarbons found here are also typical products in the flames of hydrocarbons [86].

3.2. Density changes of reacting flows

Volume expansion factors (ε) and effective residence times (τ_{eff}) at various pressures are presented along with the density change neglected residence times (τ) in Table 1. ε values are larger than 1 with increasing τ for ethylene and propylene experiments, implying that these hydrocarbons principally undergo decomposition reactions leading to an increase in the total numbers of gas phase species. The ε values in propylene experiments are larger than those in ethylene, indicating that the extent of propylene decomposition is more extensive than in the case of ethylene. The ε values in the propylene experiments decrease with increasing pressure, suggesting that decomposition reactions are overlapped by combination reactions being favored at increasing pressures. Unlike these, the ε values of acetylene are less than 1 and decrease with both increasing pressure and τ. Benzene formation by the combination of three acetylene moieties should be responsible for the density increase, making τ_{eff} longer.

3.3. Material balances and product distributions

Product distributions as well as total carbon yields (material balances) are summarized in Table 2. The yields are calculated based on C_1. The complete sets of the observed species yields are included in the Supplementary data. Gaseous products are distinguished into CH_4, C_2, C_3, and C_4 hydrocarbons, and condensing products are distinguished into benzene and other aromatic hydrocarbons (AHs). Yields of carbon deposited on the substrate were calculated based on the data in our previous study in which the weights of carbon deposited on the substrates were measured [82]. Total carbon yields are generally in the range from 90% to 100%. Carbon deposited outside the substrate and unidentified products account for missing carbon. Total carbon yields slightly higher than 100% may be attributed to experimental errors. In the ethylene experiments the carbon balance is less perfect, especially at lower pressures and longer residence times. The reason may be polymerization products that are formed by thermal polymerization of ethylene [87]. The majority of these polyene compounds would stick to the inner wall of the tubes from which the products were not recovered. Benzene is a major product and comprising much of total condensing products for all precursor hydrocarbons. Yields of benzene and aromatic hydrocarbons increase with increasing pressure and residence time. The yields of deposited carbon are as low as 1–2% for ethylene and propylene. Pressure has a little effect on the carbon yields. On the other hand, the yields of deposited carbon in the CVD from acetylene increase up to 8.9% with an increase in residence time and pressure. The difference in the yields of deposited carbon should result from different carbon to

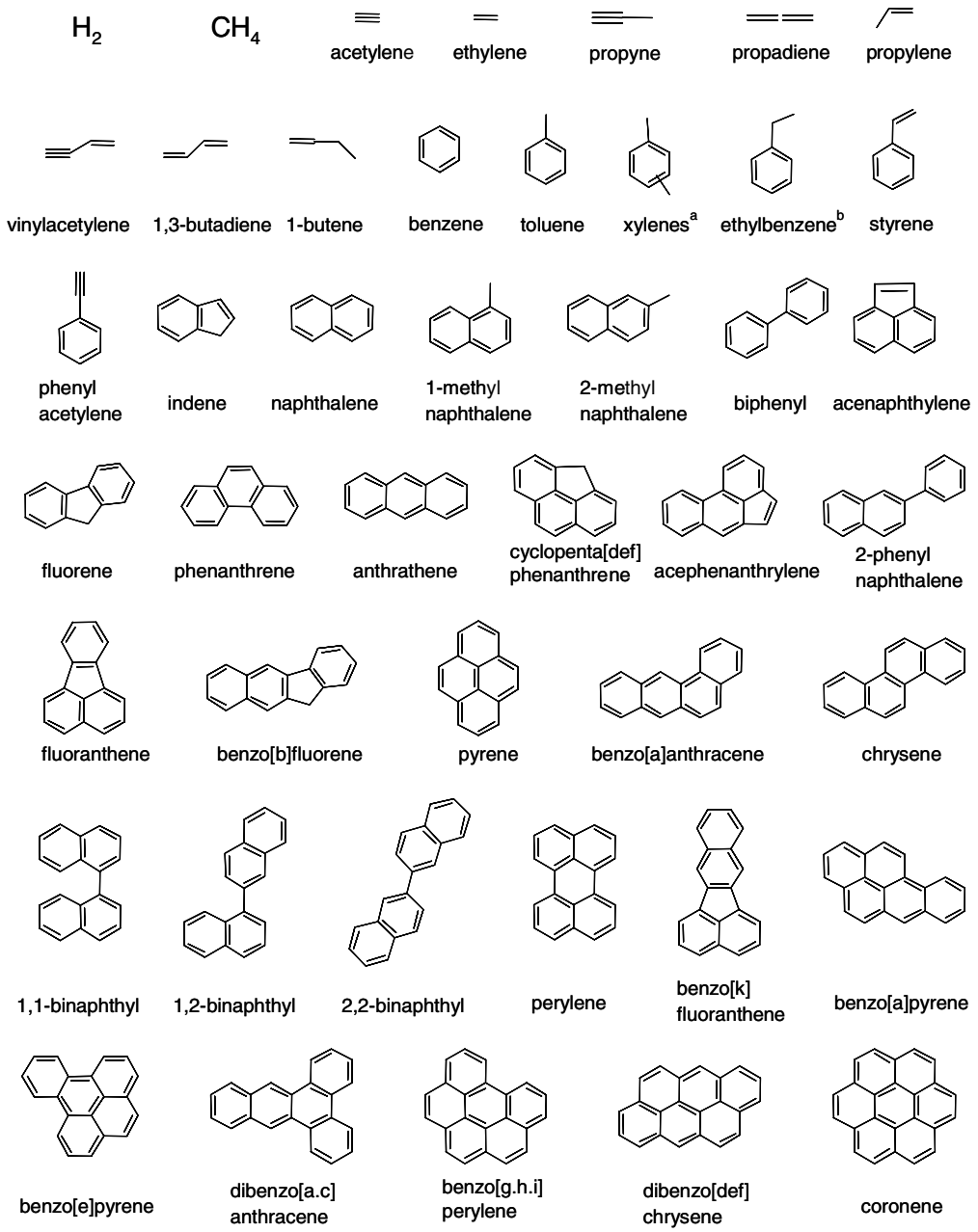

Fig. 1. Compounds found in gas phase in CVD of carbon from ethylene, acetylene, and propylene at 900 °C. (a) *o*-, *m*-, *p*-xylenes are not distinguished. (b) Not distinguished from xylenes peaks.

hydrogen ratios of 0.5 (ethylene and propylene) and 1 (acetylene). Hydrogen plays an important role in carbon deposition [88], as it inhibits carbon deposition by blocking active sites, mainly existing at the edges of graphene layers, as a consequence of forming carbon-hydrogen complexes. These results imply that the carbon deposition rate is not simply correlated with the concentration of aromatic hydrocarbons in the gas phase.

3.4. Ethylene pyrolysis

Fig. 2 shows unconverted ethylene as well as product yields in % (based on C_1 for hydrocarbons and H_1 for hydrogen) in CVD of carbon from ethylene at 8 kPa and 900 °C. Ethylene, hydrogen, 1,3-butadiene, methane, acetylene, and benzene are the major compounds. The yield of 1,3-butadiene exhibits a maximum at around 0.4 s whereas the yields of other products increase with increasing τ_{eff}. Possible routes to major products are discussed briefly based on the literature and our recent study of the detailed chemical kinetic modeling of the hydrocarbon pyrolysis [89]. Dehydrogenative decomposition of ethylene is a possible reaction to form hydrogen and acetylene [49]. 1,3-butadiene should be formed principally by combination of ethylene and vinyl radical (C_2H_3) [49], and converts into consecutive products. Reaction of 1,3-butadiene with vinyl

Table 1
Prescribed residence time (τ), volume expansion factor (ε), and effective residence time (τ_{eff}) in CVD experiments at 900 °C

Precursor	p, kPa	τ, s	ε, –	τ_{eff}, s
C_2H_4 (ethylene)	2	0.25	1.00	0.25
		0.50	1.02	0.49
		0.75	1.05	0.71
		1.00	1.09	0.92
	4	0.25	1.02	0.24
		0.50	1.03	0.48
		0.75	1.07	0.70
		1.00	1.11	0.90
	8	0.25	1.06	0.24
		0.50	1.05	0.47
		0.75	1.05	0.71
		1.00	1.05	0.95
	15	0.25	1.06	0.24
		0.50	1.08	0.46
		0.75	1.09	0.69
		1.00	1.08	0.93
C_2H_2 (acetylene)	2	0.25	1.00	0.25
		0.50	1.00	0.50
		0.75	1.00	0.75
		1.00	0.99	1.01
	4	0.25	1.00	0.25
		0.50	0.99	0.51
		0.75	0.94	0.80
		1.00	0.90	1.11
	8	0.25	0.94	0.27
		0.50	0.90	0.56
		0.75	0.88	0.85
		1.00	0.85	1.18
	15	0.25	0.73	0.34
		0.50	0.64	0.78
		0.75	0.61	1.23
		1.00	0.61	1.64
C_3H_6 (propylene)	2	0.10	1.09	0.09
		0.25	1.29	0.19
		0.50	1.65	0.30
		0.75	1.90	0.39
		1.00	2.17	0.46
	4	0.12	1.07	0.11
		0.25	1.23	0.20
		0.50	1.37	0.36
		0.75	1.61	0.47
		1.00	1.72	0.58
	8	0.12	1.07	0.11
		0.25	1.23	0.20
		0.50	1.42	0.35
		0.75	1.55	0.48
		1.00	1.64	0.61
	15	0.25	1.20	0.21
		0.50	1.37	0.36
		0.75	1.51	0.50
		1.00	1.58	0.63

radical produce linear C_6 species [90] which further convert into benzene [91,92]. Possible routes to explain methane formation are ethyl radical (C_2H_5) decomposition [93] and isomerization of 1,3-butadiene to 1,2-butadiene followed by decomposition into methyl (CH_3) and propargyl (C_3H_3) [94]. Dimerization of propagyls is also known to be an important route to benzene [95]. Decomposition of 1-butene which is not observed in this study but detected in other studies [12,13,16,25] yields methyl and allyl (C_3H_5) and considered as a possible pathway in methane formation.

3.5. Acetylene pyrolysis

Fig. 3 shows uncoverted acetylene as well as product yields in % (based on C_1 for hydrocarbons and H_1 for hydrogen) in CVD of carbon from acetylene at 8 kPa and 900 °C. Benzene, hydrogen, vinylacetylene, naphthalene, ethylene, and methane are major products. The yield of vinylacetylene exhibits a maximum at around 0.2 s whereas the yields of other products increase with increasing τ_{eff}. Hydrogen should be formed by direct formation of pyrolytic carbon from acetylene and formation of PAHs. Dimerization of acetylene yields vinylacetylene [96]. Benzene is mainly formed by combination of acetylene and vinylacetylene [97]. Addition of vinylacetylene to benzene is a possible route in naphthalene formation [98]. In addition to the molecular paths, radical paths involving C_4H_5 and C_4H_3 are also important especially at high temperatures [41,99]. Substantial amount of methane should be formed from impurity such as acetone in the acetylene feedstock [47]. Acetone produces methyl radicals that are known to play an important role in branching chain reactions.

3.6. Propylene pyrolysis

Fig. 4 shows unconverted propylene as well as product yields in % (based on C_1 for hydrocarbons and H_1 for hydrogen) in CVD of carbon from propylene at 8 kPa and 900 °C. Methane, acetylene, hydrogen, benzene, ethylene, propyne, 1,3-butadiene, and propadiene are major products. The yields of propyne, 1,3-butadiene, and propadiene exhibit maxima at $0.1 \sim 0.2$ s whereas the yields of other products increase with increasing τ_{eff}. Methane and ethylene should be formed by α-scission of propylene [73]. β-scission of propylene yields allyl radical (C_3H_5) [72], which is further converted into propadiene [72]. Propyne should be mainly formed by the isomerization of propadiene [100]. These C_3 compounds as well as propargyl radical should play a major role in benzene formation [100].

3.7. Influence of pressure

The influence of pressure on the conversion of the hydrocarbons is investigated to determine global reaction orders which may provide some information on the reaction mechanism. Fig. 5 shows uncoverted amounts in % of ethylene, acetylene, and propylene as a function of the effective residence time at a temperature of 900 °C and various pressures. The conversion of all hydrocarbons increases continuously with increasing τ_{eff}; increasing pressure has a strongly accelerating effect on the conversion of all hydrocarbons, most significantly in the case of acetylene. The

Table 2
Product distributions (in %, C_1 base) in CVD experiments at 900 °C

Precursor	p, kPa	τ_{eff}, s	CH_4	C_2	C_3	C_4	Benzene	AHs[a]	PyC[b]	Total
C_2H_4 (ethylene)	2	0.25	0.44	88.9	0.3	3.9	0.4	0.1	1.6	95.7
		0.49	0.77	82.4	0.4	4.3	1.1	0.3	1.9	91.2
		0.71	1.01	76.5	0.5	4.3	1.7	0.4	2.2	86.7
		0.92	1.28	74.2	0.5	4.4	2.2	1.1	2.5	86.1
	4	0.24	0.42	87.5	0.6	6.1	0.7	0.4	1.1	96.8
		0.48	0.88	80.2	0.8	6.4	1.5	1.1	1.3	92.1
		0.70	1.16	74.4	0.8	6.1	2.7	1.9	1.6	88.7
		0.90	1.57	71.5	0.7	5.4	2.9	2.6	1.9	86.6
	8	0.24	0.88	88.3	0.8	5.6	0.9	0.4	0.9	97.7
		0.47	1.75	78.8	1.0	7.0	2.0	1.2	1.1	92.8
		0.71	2.47	72.1	0.9	6.2	3.9	3.1	1.3	90.1
		0.95	3.25	67.7	0.9	5.8	7.0	4.9	1.5	91.1
	15	0.24	1.51	84.3	1.2	7.7	2.5	0.9	0.7	99.0
		0.46	2.77	74.8	1.1	6.6	5.1	2.2	0.9	93.5
		0.69	3.87	68.8	1.1	6.0	8.3	3.7	1.1	92.8
		0.93	4.67	63.1	1.0	5.4	14.2	6.3	1.4	95.9
C_2H_2 (acetylene)	2	0.25	0.12	94.8	1.1	1.0	0.7	0.7	1.4	99.7
		0.50	0.31	94.3	0.8	0.8	0.7	0.9	1.6	99.5
		0.75	0.38	94.0	0.6	0.8	0.8	1.1	1.7	99.4
		1.01	0.46	92.5	0.6	0.7	0.9	1.5	1.8	98.4
	4	0.25	0.18	90.0	1.0	2.5	1.2	2.0	1.9	98.8
		0.51	0.51	84.6	0.8	2.5	1.5	2.6	2.1	94.5
		0.80	0.45	79.4	0.7	2.4	2.8	3.8	2.3	91.9
		1.11	0.58	75.2	0.5	2.0	4.7	5.8	2.6	91.4
	8	0.27	0.32	83.0	1.0	4.0	6.8	3.6	3.0	101.7
		0.58	0.51	70.7	0.8	3.5	13.3	5.1	3.7	97.5
		0.85	0.74	62.0	0.6	2.6	18.7	6.9	4.4	95.9
		1.18	1.03	53.1	0.3	2.4	22.1	12.4	5.5	96.8
	15	0.34	0.54	59.2	1.0	2.9	17.8	9.1	2.7	93.2
		0.78	1.11	41.7	0.8	1.9	28.0	14.8	3.5	91.7
		1.23	1.65	33.2	0.5	1.4	29.3	16.3	5.3	87.8
		1.64	2.11	27.7	0.3	1.2	32.6	19.6	8.9	92.3
C_3H_6 (propylene)	2	0.09	1.70	4.0	95.9	2.4	n.d.	n.d.	n.d.	n.d.
		0.19	3.72	7.8	78.7	3.3	2.1	0.5	1.3	97.4
		0.30	7.42	15.2	60.1	3.4	2.2	2.6	1.6	92.4
		0.39	10.87	18.1	50.3	4.1	3.2	5.7	1.9	94.2
		0.46	12.79	21.0	42.5	4.1	3.6	4.2	2.2	90.4
	4	0.11	2.33	4.9	86.3	2.6	n.d.	n.d.	n.d.	n.d.
		0.20	5.86	11.0	71.4	3.2	4.0	2.7	1.2	99.4
		0.36	9.35	15.9	47.0	2.8	11.0	7.6	1.6	95.1
		0.47	12.63	20.7	35.3	3.3	13.4	9.0	1.9	96.1
		0.58	14.60	22.9	25.5	2.8	18.8	12.4	2.3	99.3
	8	0.11	3.26	6.6	75.1	3.7	n.d.	n.d.	n.d.	n.d.
		0.20	6.97	13.1	58.7	4.1	8.2	4.1	0.9	96.1
		0.35	11.24	19.3	32.1	3.4	18.0	9.4	1.2	94.6
		0.48	13.98	22.9	19.6	3.2	22.8	13.2	1.5	97.1
		0.61	15.38	24.7	14.4	3.0	24.8	16.5	1.8	100.6
	15	0.21	8.59	15.0	45.5	3.6	10.8	5.5	0.9	89.9
		0.36	10.71	22.0	18.3	3.1	19.9	13.5	1.2	88.7
		0.50	16.66	25.5	9.3	2.8	23.0	16.4	1.5	95.1
		0.63	18.69	27.2	5.9	2.8	29.5	16.6	1.9	102.6

[a] Aromatic hydrocarbons except for benzene.
[b] Pyrolytic carbon deposited on substrate.

accelerating effect of pressure indicates that reactions with an order higher than one are included in the conversion of the hydrocarbons.

3.8. Global reaction order and dominant reactions

Reaction orders are determined for the formal reaction:

Precursor hydrocarbon → Products

Fractional life method [101] is used to approximate the reaction order. This method is based on

$$t_F = \frac{F^{1-n} - 1}{k(n-1)} C_{i0}^{1-n} \tag{5}$$

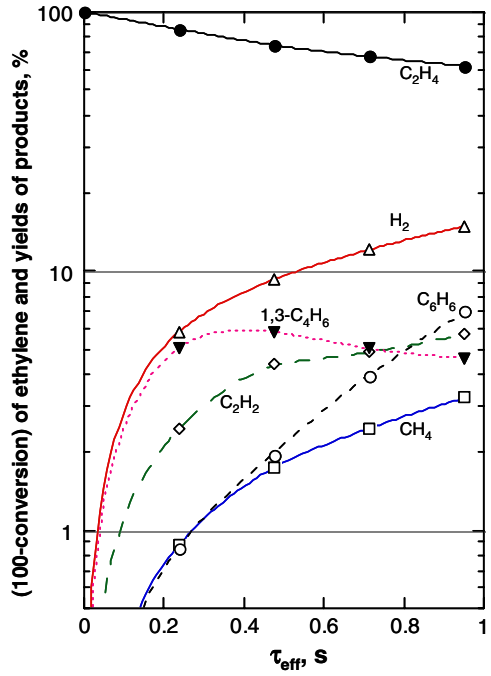

Fig. 2. Product yields and (100-conversion) of ethylene vs τ_{eff} in CVD of carbon from ethylene at 900 °C and 8 kPa. Yields are based on C_1 and H_1 for hydrocarbons and hydrogen, respectively.

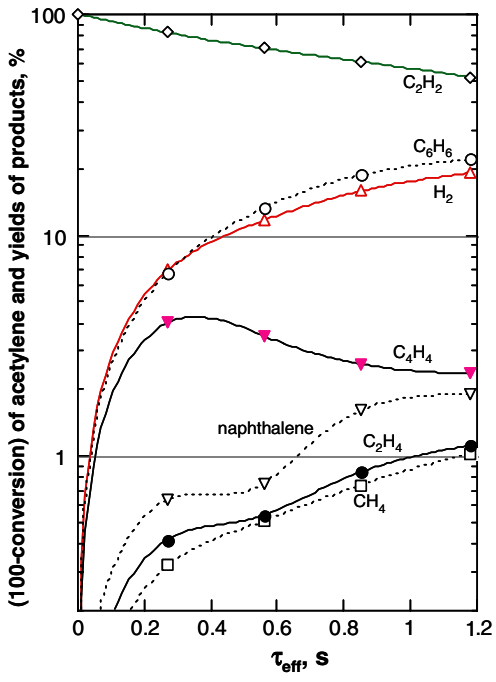

Fig. 3. Product yields and (100-conversion) of acetylene vs τ_{eff} in CVD of carbon from acetylene at 900 °C and 8 kPa. Yields are based on C_1 and H_1 for hydrocarbons and hydrogen, respectively.

where t_F is the time needed for the concentration of reactants to drop to the fractional value of F, k is the global rate constant, n is the reaction order ($\neq 1$), C_{i0} is the initial concentration of species i. Values of t_F are determined at F

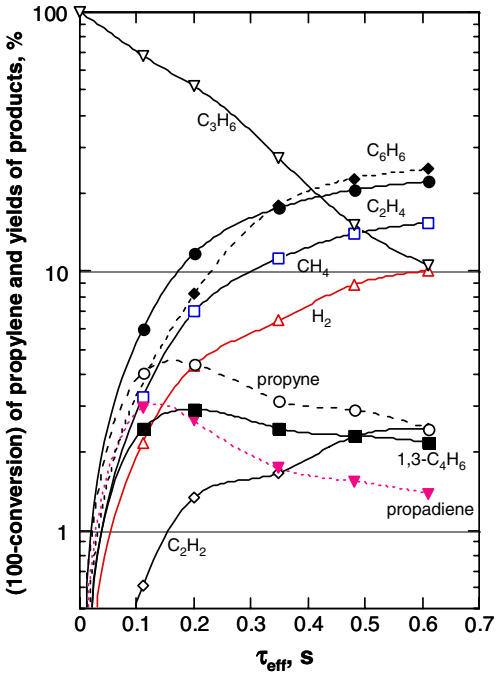

Fig. 4. Product yields and (100-conversion) of propylene vs τ_{eff} in CVD of carbon from propylene at 900 °C and 8 kPa. Yields are based on C_1 and H_1 for hydrocarbons and hydrogen, respectively.

values of 0.7, 0.8, and 0.6 for ethylene, acetylene, and propylene, respectively. An nth order rate equation is described by

$$C_i^{1-n} - C_{i0}^{1-n} = k(n-1)\tau_{eff} \quad (6)$$

where C_i is the concentration of species i at τ_{eff}. Eq. (6) is used to examine whether k is independent of the initial pressure.

Plots based on Eq. (5), that is $\log t_F$ vs $\log C_{i0}$, give straight lines of which slopes correspond to $(n-1)$ (see the Supplementary data). n values were determined to be 1.2 (ethylene), 2.7 (acetylene), and 1.5 (propylene). Previous studies of ethylene pyrolysis showed that the ethylene consumption rate is first order in the ethylene concentration [9,11]. The overall reaction order of propylene destruction evaluated here ($n = 1.5$) also agrees well with previous works by Kallend et al. ($n = 1.4$) [61] and Kunigi et al. ($n = 1.5$) [63]. However the reaction order of acetylene consumption is 2.7 which is higher than second order which seem most assured in the literatures [34,38]. Using these n values, plots based on Eq. (6), that is C_i^{1-n} vs τ_{eff}, are made and given in the Supplementary data. The plots can be approximated by straight lines with almost same slopes in the case of ethylene and acetylene, but not of propylene. Averaged k-values resulting from the slopes of the straight lines of these plots are 0.55 and 1.5 for ethylene and acetylene, respectively. The data of acetylene at the lowest pressure of 2 kPa were canceled in averaging k because of their obvious deviations.

For ethylene, n is 1.2 and k is independent of p. The lines drawn in Fig. 5 (upper) are based on Eq. (6) using the

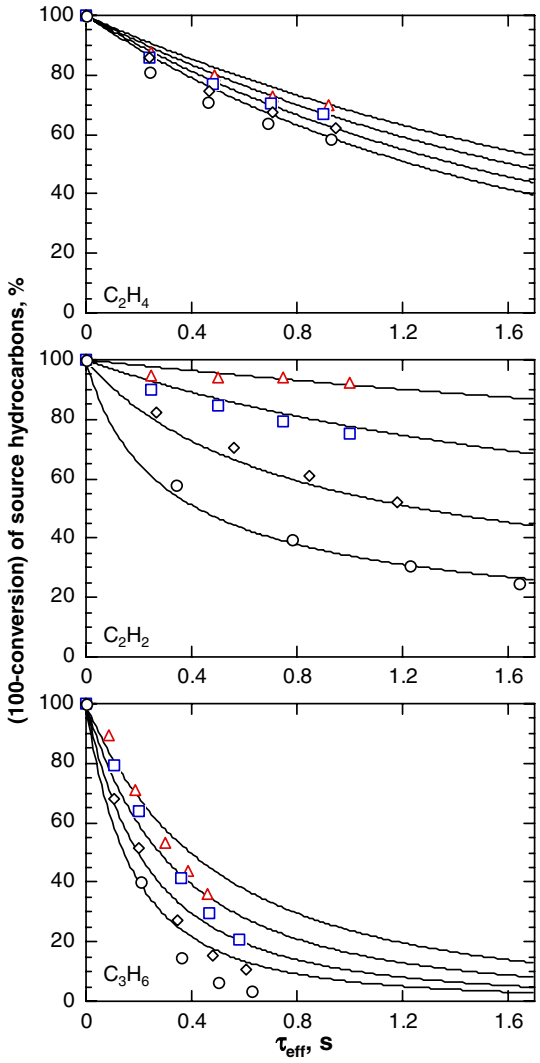

Fig. 5. Consumption of source hydrocarbons in CVD of carbon from ethylene(upper), acetylene(middle), and propylene(lower) at 900 °C and pressures of 2 (△), 4 (□), 8 (◇), 15 (○) kPa. The solid lines were calculated based on a single formal reaction for ethylene ($n = 1.2$, $k = 0.55$) and acetylene ($n = 2.7$, $k = 1.5$), and propylene ($n = 1.5$, $k = 4.6$).

values of $n = 1.2$ and $k = 0.55$; they show good agreement with the experiments. This result suggests that the overall reaction is dominated by first order decomposition reactions [17,20] such as

$$C_2H_4 \rightarrow C_2H_3 + H$$
$$C_2H_4 \rightarrow C_2H_2 + H_2$$

A superimposed bimolecular reaction [10],

$$C_2H_4 + C_2H_4 \rightarrow C_2H_5 + C_2H_3$$

should be responsible for a slightly higher reaction order of $n = 1.2$.

For acetylene, n is 2.7 and k is almost independent of p except for the data at 2 kPa. The lines in Fig. 5(middle) are also based on Eq. (6) using values of $n = 2.7$ and $k = 1.5$. A good agreement with the experimental data is achieved within the range of conditions tested. This suggests a trimerization reaction ($n = 3$) of acetylene

$$3C_2H_2 \rightarrow C_6H_6$$

to be the dominating reaction. This result agrees with conclusions of an earlier study [4]. This molecular polymerization represents an overall reaction, in which actually several fragment radical chain steps are included as found by Kieffer et al. [49].

For propylene, plots based on Eq. (5) show that linear approximations are limited to short τ_{eff}. The deviations from linearity become more significant at increasing pressure. Linear approximations were made for short τ_{eff} to determine the k values at all pressures. Using the averaged k of 4.6, $n = 1.5$, and the Eq. (6) the lines in Fig. 5 (lower) are obtained. A satisfying agreement at short τ_{eff} suggests simultaneously occurring first order and second order reactions in an initial stage of propylene pyrolysis. The first order reactions should include the decomposition reactions such as

$$C_3H_6 \rightarrow C_3H_5 + H$$
$$C_3H_6 \rightarrow C_2H_3 + CH_3$$

The reported rate constants of the above two first order decomposition reactions are 0.18 s^{-1} (β-scission) [72] and 0.03 s^{-1} (α-scission) [73] at 900 °C, implying that the first reaction is clearly privileged. The second order reactions like the bimolecular reaction [65],

$$C_3H_6 + C_3H_6 \rightarrow C_3H_5 + C_3H_7$$

should occur in parallel. Expected differences between calculations and experiments, observed at longer τ_{eff}, are attributed to additional second order reactions. Simon et al. [65] found that the formation rates of 1,3-butadiene, cyclopentadiene and C_6 compounds are second order with respect to propylene initial concentration. This indicates that reactions between propylene and primary reaction products or between primary products leading to C_4, C_5, and C_6 compounds become more significant at longer residence times.

4. Conclusions

The product composition in CVD of pyrolytic carbon from ethylene, acetylene, and propylene was analyzed at 900 °C. More than 40 compounds were identified and quantitatively determined as a function of residence time up to 1.6 s and pressures varying from 2 to 15 kPa. Material balances show that more than 90% of carbon could be detected in the experiments, providing a useful experimental database for kinetic modeling studies of gas phase reactions with detailed chemistry [89]. Global kinetic analysis of the conversion of the precursor hydrocarbons provided insight into the decisive reactions occurring in the gas phase, being a first step in the development of a detailed kinetic model based on elementary reactions.

Acknowledgements

This research was conducted in the Sonderforschungsbereich (SFB) 551 "Carbon from gas-phase: elementary reactions, structures, materials," which is funded by the

Deutsche Forschungsgemeinschaft (DFG). The Alexander von Humboldt Foundation is acknowledged for providing a research fellowship to KN.

Appendix A. Supplementary data

Supplementary data associated with this article can be found, in the online version, at doi:10.1016/j.carbon.2005.12.050.

References

[1] Golecki I. Industrial carbon chemical vapor infiltration (CVI) processes. In: Delhaes P, editor. World of carbon. Fibers and composites, vol. 2. London and New York: Taylor & Francis; 2003. p. 112–38.
[2] Hüttinger KJ. CVD in hot wall reactors—the interaction between homogeneous gas-phase and heterogeneous surface reactions. Chem Vapor Deposition 1998;4(4):151–8.
[3] Hüttinger KJ. Fundamentals of chemical vapor deposition in hot wall reactors. In: Delhaes P, editor. World of carbon. Fibers and composites, vol. 2. London and New York: Taylor & Francis; 2003. p. 75–86.
[4] Becker A, Hüttinger KJ. Chemistry and kinetics of chemical vapor deposition of pyrocarbon—II. Pyrocarbon deposition from ethylene, acetylene and 1,3-butadiene in the low temperature regime. Carbon 1998;36(3):177–99.
[5] Zhang WG, Hüttinger KJ. Chemical vapor infiltration of carbon—revised. Part I: Model simulations. Carbon 2001;39(7):1013–22.
[6] Zhang WG, Hüttinger KJ. Simulation studies on chemical vapor infiltration of carbon. Compos Sci Technol 2002;62(15):1947–55.
[7] Skinner GB, Sokoloski EM. Shock tube experiments on the pyrolysis of ethylene. J Phys Chem 1960;64(8):1028–31.
[8] Tsang W, Waelbroeck F, Bauer SH. Kinetics of production of C2 during pyrolysis of ethylene. J Phys Chem 1962;66(2):282–7.
[9] Gay ID, Kern RD, Kistiako Gb, Niki H. Pyrolysis of ethylene in shock waves. J Chem Phys 1966;45(7):2371–7.
[10] Benson SW, Haugen GR. Mechanisms for some high-temperature gas-phase reactions of ethylene acetylene and butadiene. J Phys Chem 1967;71(6):1735–46.
[11] Homer JB, Kistiako Gb. Oxidation and pyrolysis of ethylene in shock waves. J Chem Phys 1967;47(12):5290–5.
[12] Halstead MP, Quinn CP. Pyrolysis of ethylene. Trans Faraday Soc 1968;64(541P):103–8.
[13] Simon M, Back MH. Kinetics of thermal reactions of ethylene. Canad J Chem 1969;47(2):251–5.
[14] Roth P, Just T. Measurements on homogeneous thermal decay of ethylene. Phys Chem Chem Phys 1973;77(12):1114–8.
[15] Cundall RB, Fussey DE, Harrison AJ, Lampard D. Shock-tube studies of high-temperature pyrolysis of acetylene and ethylene. J Chem Soc Faraday Trans I 1978;74:1403–9.
[16] Back MH, Martin R. Thermal-reactions of ethylene at 500 °C in the presence and absence of small quantities of oxygen. Int J Chem Kin 1979;11(7):757–74.
[17] Tanzawa T, Gardiner WC. Thermal-decomposition of ethylene. Combust Flame 1980;39(3):241–53.
[18] Ayranci G, Back MH. Kinetics of the bimolecular initiation process in the thermal-reactions of ethylene. Int J Chem Kin 1981;13(9):897–911.
[19] Koike T, Morinaga K. Shock-tube studies of the acetylene and ethylene pyrolysis by UV absorption. Bull Chem Soc Japan 1981;54(2):530–4.
[20] Kiefer JH, Kapsalis SA, Alalami MZ, Budach KA. The very high-temperature pyrolysis of ethylene and the subsequent reactions of product acetylene. Combust Flame 1983;51(1):79–93.
[21] Mackenzie AL, Pacey PD, Wimalasena JH. Induction periods in the formation of ethane from the pyrolysis of ethylene. Canad J Chem—Revue Canad Chim 1983;61(9):2033–6.
[22] Mackenzie AL, Pacey PD, Wimalasena JH. Radical-addition, decomposition, and isomerization-reactions in the pyrolysis of ethane and ethylene. Canad J Chem—Revue Canad Chim 1984;62(7):1325–8.
[23] Jayaweera IS, Pacey PD. The formation of hydrogen in ethylene pyrolysis at 900 K. Int J Chem Kin 1988;20(9):719–29.
[24] Dagaut P, Boettner JC, Cathonnet M. Ethylene pyrolysis and oxidation—a kinetic modeling study. Int J Chem Kin 1990;22(6):641–64.
[25] Roscoe JM, Jayaweera IS, Mackenzie AL, Pacey PD. The mechanism of ethylene pyrolysis at small conversions. Int J Chem Kin 1996;28(3):181–93.
[26] Hidaka Y, Nishimori T, Sato K, Henmi Y, Okuda R, Inami K, et al. Shock-tube and modeling study of ethylene pyrolysis and oxidation. Combust Flame 1999;117(4):755–76.
[27] Krestinin AV. Detailed modeling of soot formation in hydrocarbon pyrolysis. Combust Flame 2000;121(3):513–24.
[28] Minkoff GJ. Excited states of acetylene and their role in pyrolysis. Canad J Chem—Revue Canad Chim 1958;36(1):131–6.
[29] Badger GM, Lewis GE, Napier IM. The formation of aromatic hydrocarbons at high temperatures. 8. The pyrolysis of acetylene. J Chem Soc 1960:2825–7.
[30] Asaba T, Hikita T, Yoneda K. Shock tube studies on pyrolysis of lower hydrocarbons. (2) High temperature pyrolysis of acetylene. Kogyo Kagaku Zasshi 1961;64(11):1925.
[31] Cullis CF, Nettleton MA, Minkoff GJ. Infra-red spectrometric study of pyrolysis of acetylene. 1. Homogeneous reaction. Trans Faraday Soc 1962;58(474):1117–27.
[32] Cullis CF, Nettleton MA. Infra-red spectrometric study of pyrolysis of acetylene. 2. Influence of surface. Trans Faraday Soc 1963;59(482):361–8.
[33] Hou KC, Anderson RC. Comparative studies of pyrolysis of acetylene, vinylacetylene, and diacetylene. J Phys Chem 1963;67(8):1579–81.
[34] Cullis CF, Franklin NH. Pyrolysis of acetylene at temperatures from 500 to 1000 °C. Proc Royal Soc London Ser A—Math Phys Sci 1964;280(138):139–52.
[35] Fields EK, Meyerson S. A new mechanism for acetylene pyrolysis to aromatic hydrocarbons. Tetrahedron Lett 1967;8(6):571–5.
[36] Back MH. Mechanism of pyrolysis of acetylene. Canad J Chem 1971;49(13):2199–204.
[37] Beck WH, Mackie JC. Formation and dissociation of C2 from high-temperature pyrolysis of acetylene. J Chem Soc—Faraday Trans I 1975;71(6):1363–71.
[38] Ogura H. Shock-tube study on mechanism of hydrogenation and pyrolysis of acetylene. Bull Chem Soc Japan 1977;50(8):2051–7.
[39] Ogura H. Pyrolysis of acetylene behind shock-waves. Bull Chem Soc Japan 1977;50(5):1044–50.
[40] Tanzawa T, Gardiner WC. Reaction-mechanism of the homogeneous thermal-decomposition of acetylene. J Phys Chem 1980;84(3):236–9.
[41] Frenklach M, Taki S, Durgaprasad MB, Matula RA. Soot formation in shock-tube pyrolysis of acetylene, allene, and 1,3-butadiene. Combust Flame 1983;54(1–3):81–101.
[42] Duran RP, Amorebieta VT, Colussi AJ. Pyrolysis of acetylene—a thermal source of vinylidene. J Am Chem Soc 1987;109(10):3154–5.
[43] Wu CH, Singh HJ, Kern RD. Pyrolysis of acetylene behind reflected shock-waves. Int J Chem Kin 1987;19(11):975–96.
[44] Chen YQ, Jonas DM, Hamilton CE, Green PG, Kinsey JL, Field RW. Acetylene-isomerization and dissociation. Berichte Der Bunsen-Gesellschaft—Phys Chem Chem Phys 1988;92(3):329–36.
[45] Ghibaudi E, Colussi AJ. Kinetics and thermochemistry of the equilibrium 2(acetylene) = vinylacetylene—direct evidence against a chain mechanism. J Phys Chem 1988;92(20):5839–42.

[46] Kiefer JH, Mitchell KI. Molecular dissociation of vinylacetylene and its implications for acetylene pyrolysis. Energy Fuels 1988;2(4):458–61.
[47] Colket MB, Seery DJ, Palmer HB. The pyrolysis of acetylene initiated by acetone. Combust Flame 1989;75(3–4):343–66.
[48] Duran RP, Amorebieta VT, Colussi AJ. Radical sensitization of acetylene pyrolysis. Int J Chem Kin 1989;21(10):947–58.
[49] Kiefer JH, Vondrasek WA. The mechanism of the homogeneous pyrolysis of acetylene. Int J Chem Kin 1990;22(7):747–86.
[50] Benson SW. Radical processes in the pyrolysis of acetylene. Int J Chem Kin 1992;24(3):217–37.
[51] Kiefer JH, Sidhu SS, Kern RD, Xie K, Chen H, Harding LB. The homogeneous pyrolysis of acetylene. 2. The High-temperature radical chain mechanism. Combust Sci Tech 1992;82(1–6):101–30.
[52] Hidaka Y, Hattori K, Okuno T, Inami K, Abe T, Koike T. Shock-tube and modeling study of acetylene pyrolysis and oxidation. Combust Flame 1996;107(4):401–17.
[53] Dimitrijevic ST, Paterson S, Pacey PD. Pyrolysis of acetylene during viscous flow at low conversions; influence of acetone. J Anal Appl Pyrol 2000;53(1):107–22.
[54] Xu XJ, Pacey PD. An induction period in the pyrolysis of acetylene. Phys Chem Chem Phys 2001;3(14):2836–44.
[55] Xu XJ, Pacey PD. Oligomerization and cyclization reactions of acetylene. Phys Chem Chem Phys 2005;7(2):326–33.
[56] Vlasov PA, Warnatz J. Detailed kinetic modeling of soot formation in hydrocarbon pyrolysis behind shock waves. Proc Combust Inst 2003;29:2335–41.
[57] Amano A, Uchiyama M. Mechanism of pyrolysis of propylene—formation of allene. J Phys Chem 1964;68(5):1133–7.
[58] Sakakibara Y. The synthesis of methylacetylene by the pyrolysis of propylene. 1. The effect of pyrolysis conditions on product yields. Bull Chem Soc Japan 1964;37(9):1262–8.
[59] Sakakibara Y. The synthesis of methylacetylene by the pyrolysis of propylene. 2. The mechanism of the pyrolysis. Bull Chem Soc Japan 1964;37(9):1268–76.
[60] Marshall RM, Purnell JH, Shurlock BC. Initiation of propylene pyrolysis. Canad J Chem 1966;44(22):2778.
[61] Kallend AS, Purnell JH, Shurlock BC. Pyrolysis of propylene. Proc Royal Soc London Ser A—Math Phys Sci 1967;300(1460):120–39.
[62] Chappell GA, Shaw H. A shock tube study of pyrolysis of propylene. Kinetics of vinyl–methyl bond rupture. J Phys Chem 1968;72(13):4672–5.
[63] Kunugi T, Sakai T, Soma K, Sasaki Y. Thermal reaction of propylene—kinetics. Ind Eng Chem Fundamentals 1970;9(3):314–8.
[64] Kunugi T, Soma K, Sakai T. Thermal reaction of propylene-mechanism. Ind Eng Chem Fundamentals 1970;9(3):319–24.
[65] Simon M, Back MH. Kinetics of pyrolysis of propylene. 1. Canad J Chem 1970;48(2):317–25.
[66] Simon M, Back MH. Kinetics of pyrolysis of propylene. 2. Canad J Chem 1970;48(21):3313–9.
[67] Sims JA, Kershenb Ls, Shroff J. Kinetics of high-temperature pyrolysis of propylene. Ind Eng Chem Process Des Development 1971;10(2):265–71.
[68] Thrower PA, Sorg DJ. Pyrolysis of propylene over graphite substrates. Carbon 1973;11(6):672.
[69] Burcat A. Cracking of propylene in a shock-tube. Fuel 1975;54(2):87–93.
[70] Cundall RB, Fussey DE, Harrison AJ, Lampard D. High-temperature pyrolysis of ethane and propylene. J Chem Soc—Faraday Trans I 1979;75:1390–4.
[71] Kiefer JH, Alalami MZ, Budach KA. Shock-tube, laser-Schlieren study of propene pyrolysis at high-temperatures. J Phys Chem 1982;86(5):808–13.
[72] Tsang W. Chemical kinetic data-base for combustion chemistry. 5. Propene J Phys Chem Ref Data 1991;20(2):221–73.
[73] Hidaka Y, Nakamura T, Tanaka H, Jinno A, Kawano H, Higashihara T. Shock-tube and modeling study of propene pyrolysis. Int J Chem Kin 1992;24(9):761–80.
[74] Barbe P, Baronnet F, Martin R, Perrin D. Kinetics and modeling of the thermal reaction of propene at 800 K. Part III. Propene in the presence of small amounts of oxygen. Int J Chem Kin 1998;30(7):503–22.
[75] Davis SG, Law CK, Wang H. Propene pyrolysis and oxidation kinetics in a flow reactor and laminar flames. Combust Flame 1999;119(4):375–99.
[76] Goos E, Hippler H, Hoyermann K, Jurges B. Reactions of methyl radicals with propene at temperatures between 750 and 1000 K. Faraday Discussions 2001;119:243–53.
[77] Glasier GF, Pacey PD. Formation of pyrolytic carbon during the pyrolysis of ethane at high conversions. Carbon 2001;39(1):15–23.
[78] Dong GL, Hüttinger KJ. Consideration of reaction mechanisms leading to pyrolytic carbon of different textures. Carbon 2002;40(14):2515–28.
[79] Descamps C, Vignoles GL, Feron O, Langlais F, Lavenac J. Correlation between homogeneous propane pyrolysis and pyrocarbon deposition. J Electrochem Soc 2001;148(10):C695–708.
[80] Feron O, Langlais F, Naslain R. In situ analysis of gas phase decomposition and kinetic study during carbon deposition from mixtures of carbon tetrachloride and methane. Carbon 1999;37(9):1355–61.
[81] Feron O, Langlais F, Naslain R. Analysis of the gas phase by in situ FTIR spectrometry and mass spectrometry during the CVD of pyrocarbon from propane. Chem Vapor Deposition 1999;5(1):37–47.
[82] Norinaga K, Hüttinger KJ. Kinetics of surface reactions in carbon deposition from light hydrocarbons. Carbon 2003;41(8):1509–14.
[83] Zhang WGG, Hüttinger KJ. CVD of SiC from methyltrichlorosilane. Part I: Deposition rates. Chem Vapor Deposition 2001;7(4):167–72.
[84] Tischer S, Correa C, Deutschmann O. Transient three-dimensional simulations of a catalytic combustion monolith using detailed models for heterogeneous and homogeneous reactions and transport phenomena. Catal Today 2001;69(1–4):57–62.
[85] Hu ZJ, Hüttinger KJ. Influence of the surface area/volume ratio on the chemistry of carbon deposition from methane. Carbon 2003;41(8):1501–8.
[86] Bockhorn H, Fetting F, Wenz HW. Investigation of the formation of high molecular hydrocarbons and soot in premixed hydrocarbon-oxygen flames. Berichte Der Bunsen-Gesellschaft—Phys Chem Chem Phys 1983;87(11):1067–73.
[87] Neuschutz D, Zimdahl S, Zimmmermann E. Kinetics of carbon deposition by CVD from ethylene–hydrogen–argon mixtures at 1000–1100 °C and 1 bar total pressure. In: Jensen KJ, Cullen GW, editors. Proceedings of the twelfth international conference on CVD. The Electrochem Soc; 1993.
[88] Becker A, Hu Z, Hüttinger KJ. A hydrogen inhibition model of carbon deposition from light hydrocarbons. Fuel 2000;79(13):1573–80.
[89] Norinaga K, Deutechmann O. Detailed gas-phase chemistry in CVD of carbon from unsaturated light hydrocarbons. In: Proceedings of fifteenth european conference on chemical vapor deposition. Electrochemical society proceeding, vol. 2005-09, 2005. p. 348–55.
[90] Westmoreland PR, Dean AM, Howard JB, Longwell JP. Forming benzene in flames by chemically activated isomerization. J Phys Chem 1989;93(25):8171–80.
[91] Weissman M, Benson SW. Mechanism of soot initiation in methane systems. Progress Energy Combust Sci 1989;15(4):273–85.
[92] Orchard SW, Thrush BA. Photochemical studies of unimolecular processes. 6. Unimolecular reactions of C6h8 isomers and interpretation of their photolyses. Proc Royal Soc London Ser A—Math Phys Eng Sci 1974;337(1609):257–74.
[93] Tabayashi K, Bauer SH. Early stages of pyrolysis and oxidation of methane. Combust Flame 1979;34(1):63–83.
[94] Hidaka Y, Higashihara T, Ninomiya N, Masaoka H, Nakamura T, Kawano H. Shock tube and modeling study of 1,3-butadiene pyrolysis. Int J Chem Kin 1996;28(2):137–51.

[95] Wu CH, Kern RD. Shock-tube study of allene pyrolysis. J Phys Chem 1987;91(24):6291–6.
[96] Duran RP, Amorebieta VT, Colussi AJ. Lack of kinetic hydrogen isotope effect in acetylene pyrolysis. Int J Chem Kin 1989;21(9):847–58.
[97] Chanmugathas C, Heicklen J. Pyrolysis of acetylene–vinylacetylene mixtures between 400 °C and 500 °C. Int J Chem Kin 1986;18(6):701–18.
[98] Appel J, Bockhorn H, Frenklach M. Kinetic modeling of soot formation with detailed chemistry and physics: laminar premixed flames of C-2 hydrocarbons. Combust Flame 2000;121(1–2):122–36.
[99] Cole JA, Bittner JD, Longwell JP, Howard JB. Formation mechanisms of aromatic-compounds in aliphatic flames. Combust Flame 1984;56(1):51–70.
[100] Hidaka Y, Nakamura T, Miyauchi A, Shiraishi T, Kawano H. Thermal-decomposition of propyne and allene in shock-waves. Int J Chem Kin 1989;21(8):643–66.
[101] Levenspiel O. Chemical reaction engineering. John Wiley & Sons; 1999.